Applied Catalysis B: Environmental 160–161 (2014) 666–675

Contents lists available at ScienceDirect

Applied Catalysis B: Environmental

journal homepage: www.elsevier.com/locate/apcatb

Treatment of synthetic soil washing solutions containing phenanthrene and cyclodextrin by electro-oxidation. Influence of anode materials on toxicity removal and biodegradability enhancement

Emmanuel Mousset[a], Nihal Oturan[a], Eric D. van Hullebusch[a], Gilles Guibaud[b], Giovanni Esposito[c], Mehmet A. Oturan[a,*]

[a] Université Paris-Est, Laboratoire Géomatériaux et Environnement (LGE), EA 4508, UPEM, 77454 Marne-la-Vallée, France
[b] Université de Limoges, Groupement de Recherche Eau Sol Environnement (EA 4330), Faculté des Sciences et Techniques, 123 Avenue A. Thomas, 87060 Limoges Cedex, France
[c] University of Cassino and the Southern Lazio, Department of Civil and Mechanical Engineering, Via Di Biasio, 43, 03043 Cassino (FR), Italy

ARTICLE INFO

Article history:
Received 11 April 2014
Received in revised form 6 June 2014
Accepted 14 June 2014
Available online 20 June 2014

Keywords:
Polycyclic aromatic hydrocarbons (PAHs)
HPCD
Electro-Fenton
BDD anode
Bioassays

ABSTRACT

Electrochemical advanced oxidation processes were applied to treatment of highly loaded synthetic soil washing solution. Phenanthrene (PHE) and hydroxypropyl-beta-cyclodextrin (HPCD) were chosen respectively as a polycyclic aromatic hydrocarbon (PAH) representative and as a solubilizing agent. Different anode materials such as platinum (Pt), dimensionally stable anode (DSA;) and boron-doped diamond (BDD) were employed to carry out the treatment in a electrocatalytic way. Two electrochemical processes were compared: electro-Fenton (EF) and anodic oxidation (AO) with BDD as an anode. Toxicity (Microtox®) and biodegradability (BOD_5/COD) of treated solutions during the treatment were assessed.

Pt anode was found to be the most efficient one in degradation of PHE, while BDD anode showed better ability to degrade HPCD and to mineralize the solution. This confirms the different ways to treat the effluent, which are related to the O_2 evolution overpotential of selected anode: mainly electro-oxidation in the case of Pt and DSA, mineralization (conversion of organics to CO_2) mechanism in AO with BDD anode and paired electrocatalysis in the case of EF with BDD anode. Toxicity and biodegradability assays corroborate these mechanisms. After a complete degradation of PHE and HPCD corresponding to 60% mineralization of solution with EF and AO treatments using BDD as anode, the toxicity starts to decrease and the biodegradability reaches its maximal value (100%). In these conditions, the complete mineralization needs longer treatment times. But in this study electrochemical treatment is conceived to enhance the biodegradability for a biological post-treatment in a reasonably short time. Therefore six factors including energy consumptions values were compared after reaching a biodegradability of 33% and after reaching complete mineralization. Performing electrochemical treatment until reaching a BOD_5/COD ratio of 33% appears to be the best option, since EF and AO displayed most of the time a similar behaviour.

1. Introduction

Hydrophobic organic compounds (HOCs) like polycyclic aromatic hydrocarbons (PAHs) are well-known to be hazardous contaminant and their potential environmental impact and human health risk is significant [1]. Among the emerging techniques to treat them, soil washing and soil flushing appear to be cost-efficient techniques [2]. Since PAHs tend to be strongly sorbed into soil, an amphiphilic extracting agent is needed. Cyclodextrins (CDs), known as host-guest molecules, have been suggested in the last decade as an alternative to the traditional surfactants [3,4]. The derivatives of CDs are reported as having a better water-solubility and higher solubilization efficiency. Among them, hydroxypropyl-beta-cyclodextrin (HPCD) is one of the most effective CD derivative tested in soil washing experiment [5].

As soil washing/flushing process only transfers the pollutant from a solid matrix to an aqueous solution, a post-treatment of soil washing solution is required. However, these solutions represent a challenge to be treated since they are highly loaded and have

* Corresponding author. Tel.: +33 149 32 90 65; fax: +33 149 32 91 37.
E-mail addresses: mehmet.oturan@univ-paris-est.fr, oturan@univ-mlv.fr (M.A. Oturan).

http://dx.doi.org/10.1016/j.apcatb.2014.06.018
0926-3373/

most of the time a COD higher than 10,000 mg O_2 L^{-1}. Moreover, since these solutions contain many xenobiotic a biological treatment would not be efficient. Advanced oxidation processes (AOPs) [6] have been developed as alternative technologies to biological and chemical conventional processes which are inefficient in case of persistent organic pollutants (POPs) like PAHs. AOP are based on *in situ* generation of hydroxyl radical (•OH), a highly oxidizing species (E° = 2.80 V/SHE [7]). These processes are especially efficient for aromatic molecules thanks to their affinity for electrophilic aromatic substitution of hydroxyl radical which then lead to open the aromatic ring [8–11]. Among AOPs electrochemical process such as the emerging electro-Fenton (EF) process has shown promising results especially for industrial wastewaters treatments [10,12–15] and highly loaded solutions like landfill leachates [16] and reverse osmosis concentrates [17]. In this process, H_2O_2 is generated at the cathode of an electrochemical reactor from 2-electron reduction of O_2 or compressed air (Eq. (1)) while an iron catalyst (Fe^{2+}, Fe^{3+}, or iron oxides) is added to the effluent to produce •OH at the bulk acidic solution *via* Fenton's reaction (Eq. (2)):

$$O_2 + 2H^+ + 2e^- \rightarrow H_2O_2 \quad (1)$$

$$Fe^{2+} + H_2O_2 \rightarrow Fe^{3+} + HO^- + {}^\bullet OH \quad (2)$$

In contrast to the classical Fenton process, the Fenton's reagent (H_2O_2 and Fe^{2+}) is electrocatalytically *in situ* generated in the case of EF process [11,18,19], according to Eqs. (1) and (3):

$$Fe^{3+} + e^- \rightarrow Fe^{2+} \quad (3)$$

EF process is considered as a clean treatment without any production of sludge [20,21]. Furthermore, no iron would be needed for the treatment of soil washing solution, since the iron could be directly extracted from soil [22].

Another emerging electrochemical advanced oxidation process (EAOP) is the anodic oxidation (AO) [23]. This process allows generating hydroxyl radical in a catalytic way at the surface of a high O_2-overvoltage anode (M), according to Eqs. (4a) and (4b).

$$M + H_2O \rightarrow M({}^\bullet OH) + H^+ + e^- \quad (4a)$$

$$M({}^\bullet OH) + \text{organic matter} \rightarrow M + \text{oxidation products} \quad (4b)$$

The boron-doped diamond (BDD) electrode has an O_2-overvoltage of 2.3 V *vs* SHE, which is high enough to produce physisorbed hydroxyl radical BDD(•OH) through Eqs. (4a), (4b) as intermediates of water oxidation to O_2. AO with BDD as an anode material has been studied in several works [23–27]. One of the advantages of this process is that no reagents are added before or during the treatment.

Since chemical oxidation for complete mineralization is usually energy consuming treatment, combination of EAOPs with biological treatment can reduce the operating costs [28,29]. Several studies evoke AOPs as pre-treatment combined to biological post-process [30]. The most studied AOPs are Fenton [31–35], photo-Fenton and solar-photo-Fenton treatments [36–41]. According to our knowledge only few studies have reported the possibility to combine a biological post-process to an EF treatment [42–46] and an AO treatment [43,47–53]. These studies are not focused on soil washing solutions, they do not deal with PAHs pollutants and BBD anode was almost not employed during AO process. Estrada et al. [43] have shown that EF is a better option to be combined with a biological post-treatment than other treatments like chemical flocculation and electro-coagulation.

In the present paper, for the first time, we have carried out treatments of highly loaded synthetic soil washing solution by EAOPs EF and AO, by comparing the efficiency of different anode materials. Phenanthrene (PHE) that is listed among the 16 hazardous PAHs by the Environmental Protection Agency of United States (USEPA) was selected as representative soil pollutant. The solubilizing agent used in soil washing was HPCD. Pt and DSA (Ti/RuO_2-IrO_2) anodes that are known to be "active" (leading to chemisorption of •OH on surface) electrodes are compared to BDD anode, a "non-active" electrode (leading to physisorption of •OH on surface) [23,54]. In a first part of this study, the efficiency of three anodes and the two processes (EF and AO) are compared by monitoring the PHE and HPCD decay kinetics and the mineralization rate at different current intensity. A second part evokes the possibility of a biological post-treatment by following the biodegradability and evolution of the toxicity levels during the EF and AO treatments. In the last part, the different treatments with different anodes materials are compared by considering their respective energy consumptions and a multi-criteria approach.

2. Materials and methods

2.1. Chemicals

All the following products were used at analytical grade without any purification: PHE ($C_{14}H_{10}$; 178 g mol^{-1}), methanol (HPLC grade), sodium sulphate and 2-(P-toluidino)naphthalene-6-sulfonic acid sodium (TNS) were purchased from Aldrich. Heptahydrated ferrous sulfate ($FeSO_4{\cdot}7H_2O$), sulfuric acid and potassium dihydrogen phosphate (KH_2PO_4) were supplied by Acros. Hydroxypropyl-beta-cyclodextrin (HPCD; $C_{48}H_{82}O_{37}$; 1250 g mol^{-1}) was provided by Xi'an Taima Biological Engineering Company. Sodium phosphate dibasic (Na_2HPO_4), ammonium chloride (NH_4Cl), heptahydrated magnesium sulfate ($MgSO_4{\cdot}7H_2O$), dehydrated calcium chloride ($CaCl_2{\cdot}2H_2O$), D(+)-Glucose·H_2O were purchased from Merck at analytical grade. Reagents like dipotassium phosphate (K_2HPO_4), hexahydrated ferric chloride ($FeCl_3{\cdot}6H_2O$) and NaOH were provided by VWR International. Potassium chloride (KCl) and sodium sulfate (NaCl) from Fluka was used. Potassium hydrogen phthalate ($C_8H_5KO_4$) from Nicolai Tesque was employed.

Ultrapure water (UPW) from a Millipore Simplicity 185 (resistivity > 18 MΩ cm) system was used in all experiments.

All the replicates of experiments and analyses gave standard deviations below 6%.

2.2. Electrochemical cell and experiments

EF experiments were performed in a 0.40 L undivided, open and cylindrical glass electrochemical reactor at current controlled conditions. The electrochemical cell was monitored by a power supply HAMEG 7042-5. The working electrode (cathode) was a 150 cm^2 carbon-felt piece (Carbone-Lorraine). Each anode studied (Pt grid (5 cm height cylindrical and i.d. = 3 cm), DSA (Ti/RuO_2/IrO_2)) plate (5 cm × 4 cm) and BDD plate (5 cm × 4 cm)) was centred in the cell and surrounded by cathode which covered the inner wall of the cell. An electrolyte (Na_2SO_4 (Aldrich) at 0.150 M) was added to the medium in order to ensure a constant ionic strength (0.45 M). $FeSO_4{\cdot}7H_2O$ was also added at 0.2 mM as source of Fe^{2+} ion as catalyst. This concentration was determined to be optimal in a former study [55]. Prior to each experiment, the solutions were saturated in O_2 (8.53 mg O_2 L^{-1} at 22 °C) by supplying compressed air bubbling through the solution starting 10 min before the beginning of the treatment, at a flow-rate of 0.25 L min^{-1}. Solutions were stirred continuously by a magnetic stirrer. A heat exchanger system was provided to keep the solution at constant room temperature (22 °C ± 1) by using fresh water (15 °C ± 1). The pH of initial solutions was set to the optimal value of 3.0 (±0.1) by the addition of H_2SO_4 (1 M) solution. The pH changes were negligible during the electrolysis at pH 3.0; it decreased only to 2.8 (±0.1) at

the end of experiments. PHE was chosen as a PAH representative. HPCD (9 g L^{-1}) was employed to enhance the solubilization of PHE and to mimic future soil extract solutions of washing or flushing experiment [55]. Around 16 mg L^{-1} (±0.3 mg L^{-1}) equivalent to 0.09 mM of PHE was solubilized initially in each solution containing HPCD (9 g L^{-1} equivalent to 7.2 mM).

AO experiments were performed in the same electrochemical cell and conditions than EF without adding $FeSO_4{\cdot}7H_2O$ and without adjusting pH. The initial pH of the solution was equal to 6.0 (±0.1). BDD electrode (5 cm × 4 cm × 0.2 mm) was employed as anode. The same PHE (0.09 mM) with HPCD (9 g L^{-1}) solution was used.

2.3. Biodegradability tests

Respirometric methods (OECD 301F, ISO 9408) has the advantage of being a direct biological parameter of aerobic degradation in contrast to methods which measure dissolved organic carbon removal like *P. putida* bioassays or Zahn-Wellens tests [56,57]. Thus, this technique was operated to determine the Biochemical Oxygen Demand at 5 days (BOD_5) using the OxiTop® control system (WTW). An aqueous solution containing a phosphate buffer solution and a saline solution was prepared following Rodier et al. [58] procedure. This solution was then saturated in oxygen (9.1 mg O_2 L^{-1} at 20 °C) overnight. Bacteria extracted with KCl at 9 g L^{-1} (30 mL with 3 g of dried soil) and a IKA-MS1 mini-shaker (1800 rpm during 1 min) from uncontaminated soil were added just before adding the samples. All the samples were adjusted to circum-neutral pH. All the bottles containing the solutions were equipped by a rubber sleeve in which pure NaOH pellets are added to trap the CO_2 formed during biodegradation. The samples were incubated at (20 ± 0.1)°C during 5 days in dark conditions. D(+)-Glucose·H_2O was used as a reference. A blank, representing the endogenous respiration, prepared with UPW and the seed solution was done for each batch and taken into account for calculation. The BOD_5 measured in each blank was insignificant compared to the BOD_5 of the samples and causes no interference. All the BOD_5 values were confirmed by measuring the difference of dissolved oxygen at the beginning and the end of the experiment using the InoLab Oxi 730 (from WTW).

Chemical oxygen demand (COD) analyses were accomplished by a photometric method using a Spectroquant® NOVA 60 (Merck) equipment. The samples were diluted and prepared by adding 2 mL of each one in COD Cell test (15–300 mg O_2 L^{-1} range) (Merck) and by heating at 148 °C during 2 h with a Spectroquant® TR 420 (Merck). The tubes were let cool to room temperature before analysis.

Then the biodegradability was given by the ratio between BOD_5 and the COD (BOD_5/COD). Since the H_2O_2 (consumed by Fenton's reaction (Eq. (2)) as it is generated) was produced *in situ* during EF experiment and the radicals formed during EF or AO treatments have a very short life-time, these oxidants cause no interferences during the BOD_5 or COD measurements.

2.4. Toxicity assays

To assess the toxicity level of a solution, several tests with microorganisms, invertebrates, plants and fish have been developed. However, the most common one is the *Vibrio fischeri* bioluminescence inhibition assay [59]. In the aim to get data comparable to other research papers, toxicity assays of the present study were performed by using Microtox® standard method (ISO 11348-3) with marine bacteria *Vibrio fischeri* from LUMIStock LCK-487 (Hach Lange). A BERTHOLD Autolumat Plus LB 953 equipment was used. 22% of NaCl was added in each sample to ensure an osmotic protection for bacteria. Before each toxicity measurement, all the samples were adjusted to circum-neutral pH (with NaOH). Samples from EF experiments were filtered with RC filter (0.2 μm) to remove iron precipitates [60]. In each batch test, the inhibition percentage of a blank (sample without the compound studied) was measured and used for percentage of inhibition calculation based on 15 min of exposure.

2.5. Analytical determinations

2.5.1. TOC analysis

TOC analyses were performed to quantify the mineralization degree during the different kind of treatments. The solution TOC values were determined by catalytic oxidation using a Shimadzu V_{CSH} TOC analyser. All samples were acidified to pH 2 with H_3PO_4 (25%) to remove inorganic carbon. The injection volumes were 50 μL. Calibrations were performed by using potassium hydrogen phthalate solutions (50 mg C L^{-1}) as standard. All measured TOC values were given with a coefficient of variance below to 2%.

Mineralization yields (r_{min}) are considered equivalent to TOC removal percentage and are calculated according to Eq. (5):

$$r_{min}(\%) = \frac{(\Delta TOC)_t}{TOC_0} \times 100 \quad (5)$$

where $(\Delta TOC)_t$ is the difference between the initial TOC (TOC_0) and TOC at time *t*.

2.5.2. HPCD analysis

The HPCD concentration was determined by a fluorimetric technique based on enhancement of the fluorescence intensity of TNS, when it is complexed with the CD [61]. A Kontron SFM 25 spectrofluorimeter was set out at 318 nm for excitation and 428 nm for emission. Each sample was diluted in TNS (3×10^{-6} M) with a dilution factor of 200. All the measurements were done at constant temperature (22 °C ± 1). The fluorescence intensity of PHE was not significant in this range of wavelength and concentration (data not shown). Since TNS is photosensitive, TNS and the diluted samples were kept in dark conditions. This method allows quantifying HPCD and slightly modified (hydroxylated) HPCD in the same time, since the non-polar HPCD cavity brings about a TNS fluorescence intensity enhancement until the CD cavity is cleaved by the degradation technique.

2.5.3. PHE analysis

The decay of PHE was followed by reversed phase liquid chromatography (HPLC) coupled with a diode array detector from Dionex set to a wavelength of 249 nm. A reverse phase C-18 column (Purospher®, Merck) placed in an oven and set at 40.0 °C was used. The mobile phase was a mixture of water/methanol 22:78 (v/v) with a flow rate of 0.8 mL min^{-1} (isocratic mode). PHE exhibited a well-defined chromatographic peak at retention time of 6.9 min under these operating conditions. The injection volumes were 20 μL. To avoid difference of absorbance observed in the presence or absence of HPCD during analysis [62], external standards were prepared in the presence of solubilizing agent.

2.6. Energy consumption calculation

The energy consumptions are calculated according to Eqs. (6) and (7) [10]:

$$\text{Energy consumption (kWh m}^{-3}) = \frac{E_{cell} I t}{V_S} \quad (6)$$

$$\text{Energy consumption (kWh(kg TOC)}^{-1}) = \frac{E_{cell} I t}{(\Delta TOC)_t V_S} \quad (7)$$

where E_{cell} is the average cell voltage (V), I is the applied current (A), t is the electrolysis time (h), V_S is the solution volume (L) and $(\Delta TOC)_t$ is the TOC decay (g L^{-1}).

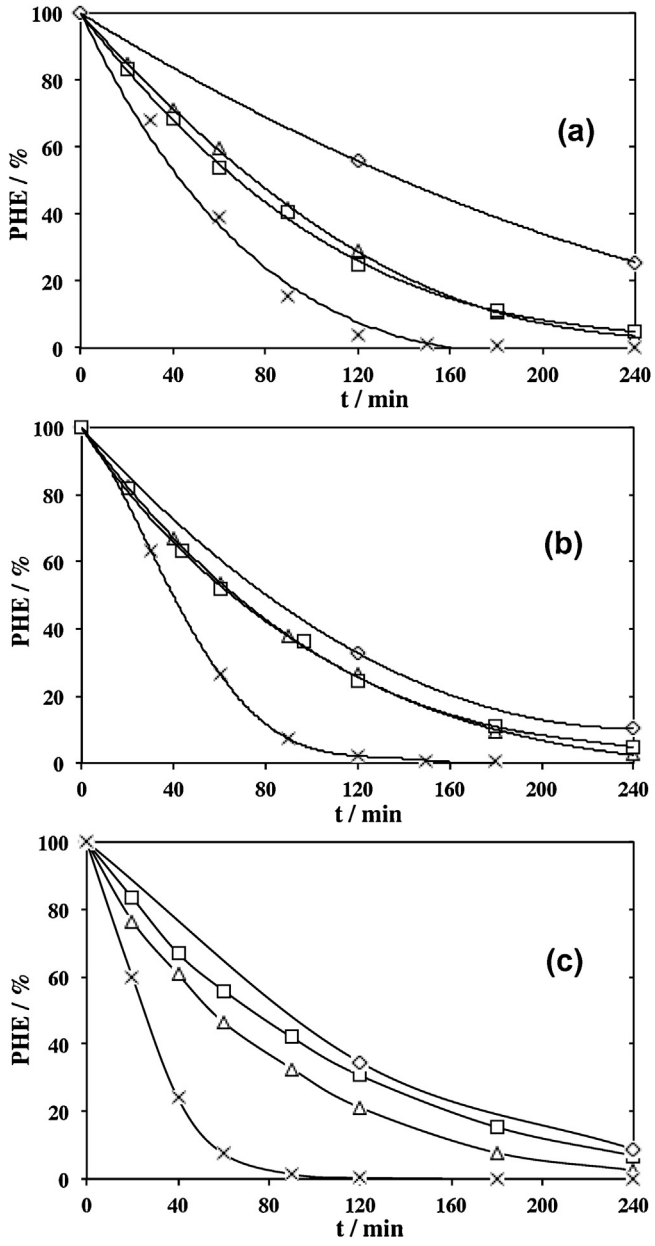

Fig. 1. Effect of applied current intensity on PHE degradation in the presence of HPCD. I (mA): (a) 500, (b) 1000 and (c) 2000 with different anode materials and different kind of treatments: (EF-Pt (×), EF-DSA (△), EF-BDD (□) and AO-BDD (◊). on [PHE] = 0.09 mM, [HPCD] = 9 g L^{-1}. EF-Pt curves from [55].

3. Results and discussion

3.1. Effect of applied current intensity on oxidation kinetics of PHE and HPCD

3.1.1. Comparison of oxidative treatments during PHE and HPCD degradations

Fig. 1 depicts the effect of applied current intensity with different anode materials (Pt, DSA and BDD) and different type of treatment (EF or AO) on PHE degradation in the presence of HPCD (9 g L^{-1}). The tested current intensities were 500, 1000 and 2000 mA. Complete degradation of PHE was not reached even after 240 min treatment by EF with DSA anode (EF-DSA), EF with BDD anode (EF-BDD) and AO with BDD (AO-BDD) processes, while complete degradation of PHE needed only 180, 150 and 90 min in EF with Pt anode (EF-Pt) at 500, 1000 and 2000 mA, respectively, in a previous study [55]. The apparent rate constants values (k_{app}) from Table 1, calculated assuming a pseudo-first order kinetic model [10], confirm that Pt anode exhibits significantly better degradation efficiency compared to EF-DSA, EF-BDD and AO-BDD treatments.

Table 1
Apparent rate constants values (k_{app}) obtained for PHE degradation (in the presence of HPCD) by EF or AO treatments, assuming pseudo-first order kinetic model.

I (A)	Process	k_{app}(PHE) (min^{-1})	R^2
PHE + HPCD			
0.5	[a]EF-Pt	0.0280 ± 0.0013	0.9937
	EF-DSA	0.0130 ± 0.0005	0.9941
	EF-BDD	0.0120 ± 0.0003	0.9953
	AO-BDD	0.0060 ± 0.0002	0.9975
PHE + HPCD			
1.0	[a]EF-Pt	0.0310 ± 0.0009	0.9956
	EF-DSA	0.0150 ± 0.0008	0.9913
	EF-BDD	0.0120 ± 0.0002	0.9978
	AO-BDD	0.0100 ± 0.0003	0.9984
PHE + HPCD			
2.0	[a]EF-Pt	0.0430 ± 0.0014	0.9940
	EF-DSA	0.0140 ± 0.0004	0.9887
	EF-BDD	0.0110 ± 0.0002	0.9969
	AO-BDD	0.0110 ± 0.0004	0.9954

[a] Values obtained from [55].

The kinetics of PHE oxidative degradation efficiency follows the rank: EF-Pt ≫ EF-DSA > EF-BDD ≈ AO-BDD, though it would be expected that EF-BDD and AO-BDD give the highest kinetic efficiency. In the case of EF-Pt, the kinetics of PHE degradation increases more rapidly (1.5 times) when the applied current increases, compared to AO-BDD. An optimal value is obtained with EF-BDD and EF-DSA at 500 mA and 1000 mA, respectively. Thus, increasing the current intensities increases the extent of competitive reactions and limits or decreases the PHE degradation efficiency. The by-products formed by oxidation of PHE as well as HPCD present in the solution can compete with PHE molecules for •OH during the oxidative process.

It appears also important to focus not only on the pollutant degradation but also on the solubilizing agent decay. Fig. 2 highlights the kinetics of HPCD degradation with the solutions described previously. The kinetics of degradation of HPCD is slower than that of PHE. This could be mainly due to the formation of a ternary complex (Fe^{2+}-HPCD-PHE) that would lead to a selective reactivity of •OH towards PHE instead of HPCD, since these radicals are formed close to PHE [55]. According to Table 2 giving apparent rate constants values of HPCD degradation (k_{app}(HPCD)), the ratio between kinetics of PHE and HPCD degradation decreases in the following sequence: EF-Pt > EF-DSA > EF-BDD > AO-BDD. These ratios

Table 2
Apparent rate constants (k_{app}) values obtained for HPCD degradation in the presence of PHE by EF or AO treatments, assuming pseudo-first order reaction kinetic model.

I (A)	Process	k_{app}(HPCD) (min^{-1})	R^2	k_{app}(PHE)/ k_{app}(HPCD)
PHE + HPCD				
0.5	EF-Pt	0.0026 ± 0.0001	0.9952	9.3
	EF-DSA	0.0034 ± 0.0002	0.9869	4.3
	EF-BDD	0.0041 ± 0.0001	0.9977	3.0
	AO-BDD	0.0042 ± 0.0001	0.9967	1.5
PHE + HPCD				
1.0	EF-Pt	0.0041 ± 0.0002	0.9927	7.7
	EF-DSA	0.0038 ± 0.0003	0.9797	3.7
	EF-BDD	0.0061 ± 0.0001	0.9978	2
	AO-BDD	0.0069 ± 0.0001	0.9991	1.4
PHE + HPCD				
12.0	EF-Pt	0.0054 ± 0.0002	0.9938	8.0
	EF-DSA	0.0054 ± 0.0002	0.9955	2.6
	EF-BDD	0.0063 ± 0.0003	0.9881	1.7
	AO-BDD	0.0085 ± 0.0005	0.9993	1.3

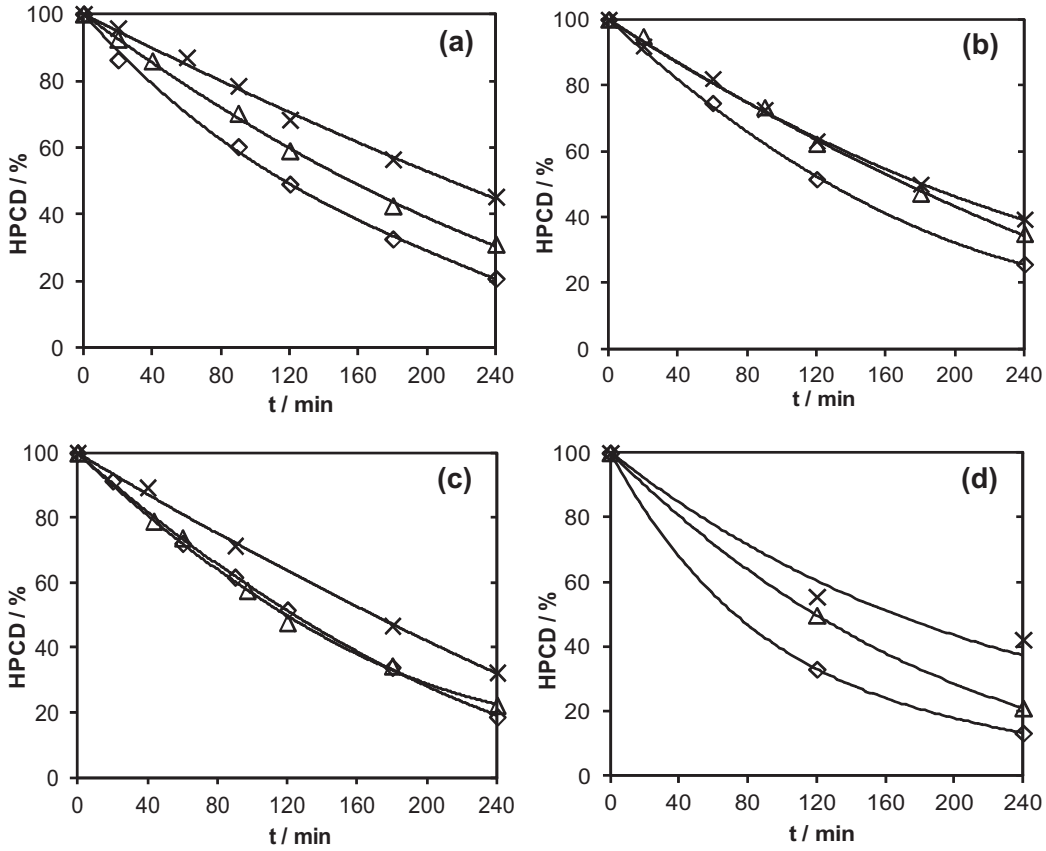

Fig. 2. Effect of applied current intensity, I (mA): 500 (×), 1000 (△) and 2000 (◊) with different anode materials and different kind of treatment: (a): EF-Pt, (b) EF-DSA, (c) EF-BDD and (d) AO-BDD.

are much lower with EF-BDD and AO-BDD treatments. On the other hand, the k_{app}(HPCD) obtained by EF-BDD and AO-BDD processes are higher than that of EF-Pt and EF-DSA treatments. At a given current intensity, when k_{app}(PHE) values decrease, k_{app}(HPCD) values increase. Thus, the k_{app}(HPCD) values are inversely correlated to the k_{app}(PHE) values, regarding the type of applied treatment. This confirms the competitive degradation between the two compounds.

It is also denoted that the k_{app}(HPCD) values increase when the applied current intensity increases in all kind of treatments.

The differences of kinetics of PHE and HPCD degradation with EF and AO treatments could be explained by the formation of ternary complex between Fe^{2+}, HPCD and PHE as already mentioned in a previous study [55]. Indeed, this ternary complex formed in EF treatment allows the direct oxidation of PHE by •OH, which accelerates the PHE degradation but slowdown the HPCD degradation.

3.1.2. Comparison of mineralization efficiency of different EAOPs treatments

The evolution of solution TOC after 4 h treatment by different EAOPs at different applied current intensity (500 mA, 1000 mA and 2000 mA) is depicted in Fig. 3. Fig. 3a shows that EF with Pt and DSA give approximately constant TOC decay yields, whatever the applied current intensity. However, treatments with BDD anodes lead to an increased mineralization yields with applied current intensity values. In all the applied current intensities, the mineralization yields after 4 h treatment followed the sequence: EF-BDD > AO-BDD ≫ EF-DSA > EF-Pt. Treatments with BDD anodes demonstrated largely better mineralization efficiency, especially at higher current intensities.

The high mineralization power of BDD compared to DSA and Pt anodes is already reported [10,23,24,54,63]. Indeed, the higher O_2-overpotential (2.3 V/SHE) at the surface of BDD allows minimizing the extent of O_2 evolution leading to the generation of heterogeneous BDD(•OH) (Eq. (4)). This allows the organic compounds to be oxidized directly at the surface of the anode (in the diffusion layer). The organic by-products that are produced close to the surface of anode are then also oxidized and so on until the final mineralization step (transformation of organics into CO_2). Thus, the initial compound is quickly mineralized in this kind of mechanism. In the meantime, the initial compound present in bulk solution is slowly degraded, *i.e.* slowly oxidized into other organic by-products. It makes the PHE degradation slower (as shown in Section 3.1.1) but the HPCD (present at a much higher concentration) degradation and the mineralization quicker, compared to EF-Pt and EF-DSA. Moreover, in the case of EF treatment with BDD anode, there are two sites for generation of •OH; one at the surface of the anode and other in the bulk solution from electrochemically generated Fenton's reagent. This is called the paired electrocatalysis process already evoked by other authors [10]. Both degradation and mineralization mechanisms take place at the same time, which could explain the better mineralization yields obtained with EF-BDD compared to AO-BDD. In the bulk solution the following reaction can occur [10] leading to a greater extent of dehydrogenated and hydroxylated derivatives through the propagation/regeneration reactions:

$$RH + {}^{\bullet}OH \rightarrow R^{\bullet} + H_2O \quad (8)$$

$$Fe^{3+} + R^{\bullet} \rightarrow R^{+} + Fe^{2+} \quad (9)$$

$$R^{+} + H_2O \rightarrow ROH + H^{+} \quad (10)$$

$$ArH + {}^{\bullet}OH \rightarrow ArH(OH)^{\bullet} \quad (11)$$

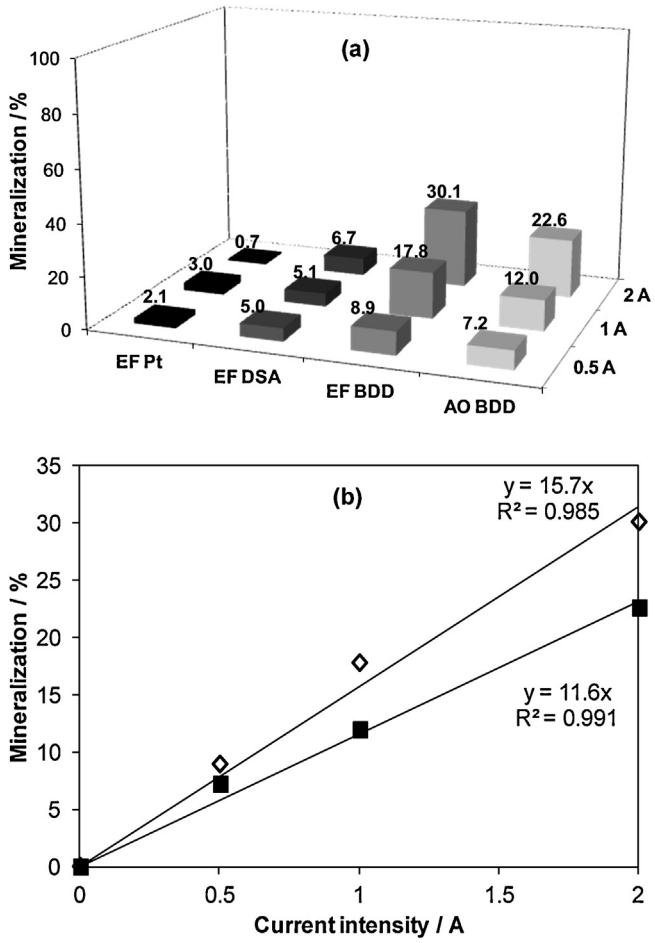

Fig. 3. Effect of applied current intensity (500 mA, 1000 mA and 2000 mA) with different anode materials and different kind of treatment on the mineralization rate obtained after 4 h of EF or AO treatments of PHE (0.09 mM) with HPCD (9 g L^{-1}) solutions. (a) EF-Pt (■), EF-DSA (■), EF-BDD (■) and AO-BDD (■); (b) evolution of mineralization degree with applied current intensity: EF-BDD (◊) and AO-BDD (■).

$$ArH(OH)^{\bullet} + O_2 \rightarrow Ar(OH) + HO_2^{\bullet} \quad (12)$$

$$HO_2^{\bullet} + H_2O_2 \rightarrow {}^{\bullet}OH + O_2 + H_2O \quad (13)$$

where RH and ArH are saturated and aromatic organics respectively, $R^{\bullet}$ and R^{+} are carboradical and carbocation respectively.

Fig. 3b denotes a linear increase of mineralization yield (r_{min}) when the current intensity (I) increases from 0 to 2000 mA with the use of BDD anode in EF process. The linear regressions give the following equations r_{min} (%) = 15.7 × I (A) (R^2 = 0.985) and r_{min} (%) = 11.6 × I (A) (R^2 = 0.991), in the case of EF-BDD and AO-BDD, respectively. EF-BDD leads to mineralization yield 1.35 times higher (in average) than with AO-BDD. This figure also demonstrates that the optimal current intensity is widely higher (≥2000 mA) by considering the TOC removal compared to degradation of PHE.

3.2. Comparison of biodegradability during PHE and HPCD oxidative treatments

The aim of electrochemical treatments applied to wastewater treatment of soil washing solutions is to degrade/mineralize different type of organic pollutants. However, sometimes the process can consume too much energy, especially when the solutions are highly loaded. Thus, it is interesting to study the evolution of biodegradability in aerobic condition of treated solution in order to use electrochemical treatment as pre-treatment for a biological post-treatment [42,44–46].

The biodegradability assays and mineralization rates during EF or AO treatments are described in Fig. 4 at a constant current intensity of 1000 mA. Mineralization data show that in each kind of treatment the mineralization increases with the treatment time. Mineralization rates during EF-BDD and AO-BDD increase largely quicker compared to EF-Pt and EF-DSA. The mineralization efficiency rank is the same as found for the effect of the applied current intensity (Section 3.1.2): EF-BDD > AO-BDD ≫ EF-DSA > EF-Pt. It can be noted that the mineralization rates are negligible during the first h of EF-Pt treatments, indicating that only oxidation mechanism occurs during this process In agreement with the highest kinetics rate constants obtained for oxidation of PHE during EF-Pt process.

Biodegradability experiments highlight also different behaviours between the treatments, though an optimal ratio can be determined in each case. First of all, The biodegradability is well enhanced in each kind of treatment, knowing that the initial biodegradability of the solution is very low ($(BOD_5/COD)_0$ = 0.1%). During the first 4 h of treatment, very low BOD_5/COD ratios are obtained during EF-BDD and AO-BDD treatments. It means that the by-products are too slowly biodegradable during this period of time. It can also be explained by the high toxicity of the solution during the first hours of treatment that is discussed in the following Section 3.3. However, the biodegradability increases very quickly between 6 h and 12 h of treatment, reaching a maximal ratio (BOD_5/COD = 100%). Regarding the EF-DSA and EF-Pt biodegradability experiments, similar behaviours are noted between both processes until 10 h treatment. BOD_5/COD ratio increases until a plateau (10%) at 2 h of treatment. Then it increases from 4 h to 10 h reaching a ratio of 33%, which indicates that the solution becomes slightly biodegradable. This ratio is the optimal value obtained for EF-DSA treatment, whereas the optimal one in EF-Pt process is largely higher (60%) after 13 h of treatment. Biodegradability with EF-Pt and EF-DSA is higher than that with EF-BDD and AO-BDD during the first 6 h treatment while they are significantly lower compared to the later processes, meaning that different degradation/mineralization kinetics are implicated during the oxidative treatments. In that way it could be assumed that different kinds of by-products are released in the bulk solution depending on the treatment (EF or AO) and the anodes (Pt, DSA or BDD). In the case of AO-BDD the intermediates products formed at the beginning of the AO treatment are directly mineralized or quickly transformed to quinone structures [10] which are strongly toxic to bacteria while oxidation of intermediates to biodegradables products occurs in solution during EF-Pt and EF-DSA processes. The previous sub-section is in agreement with these considerations.

3.3. Comparison of mineralization power of EF-BDD and AO-BDD treatments

Since Pt and DSA anodes give too low mineralization rates, only EF-BDD and AO-BDD are compared for a treatment until complete mineralization. The relation between biodegradability, HPCD degradation and the mineralization rate during EF-BDD and AO-BDD treatments is depicted in Fig. 4. The same behaviour is observed in both processes. HPCD is degraded by following a pseudo-first-order kinetics model with apparent rate constant equal to 0.56 h^{-1} and 0.37 h^{-1} in the case of EF-BDD and AO-BDD, respectively. The mineralization yield with AO-BDD (99.0%) is close to that with EF-BDD (99.7%) after 20 h of treatment and the final TOC values are 46.1 and 13.2 mg L^{-1}, respectively.

It is interesting to note that the biodegradability starts to increase only when the HPCD is almost degraded and is maximal (100%) after 12 h of treatment, *i.e.* when HPCD completely degraded. Mansour et al. (2012) [42] highlight also the same

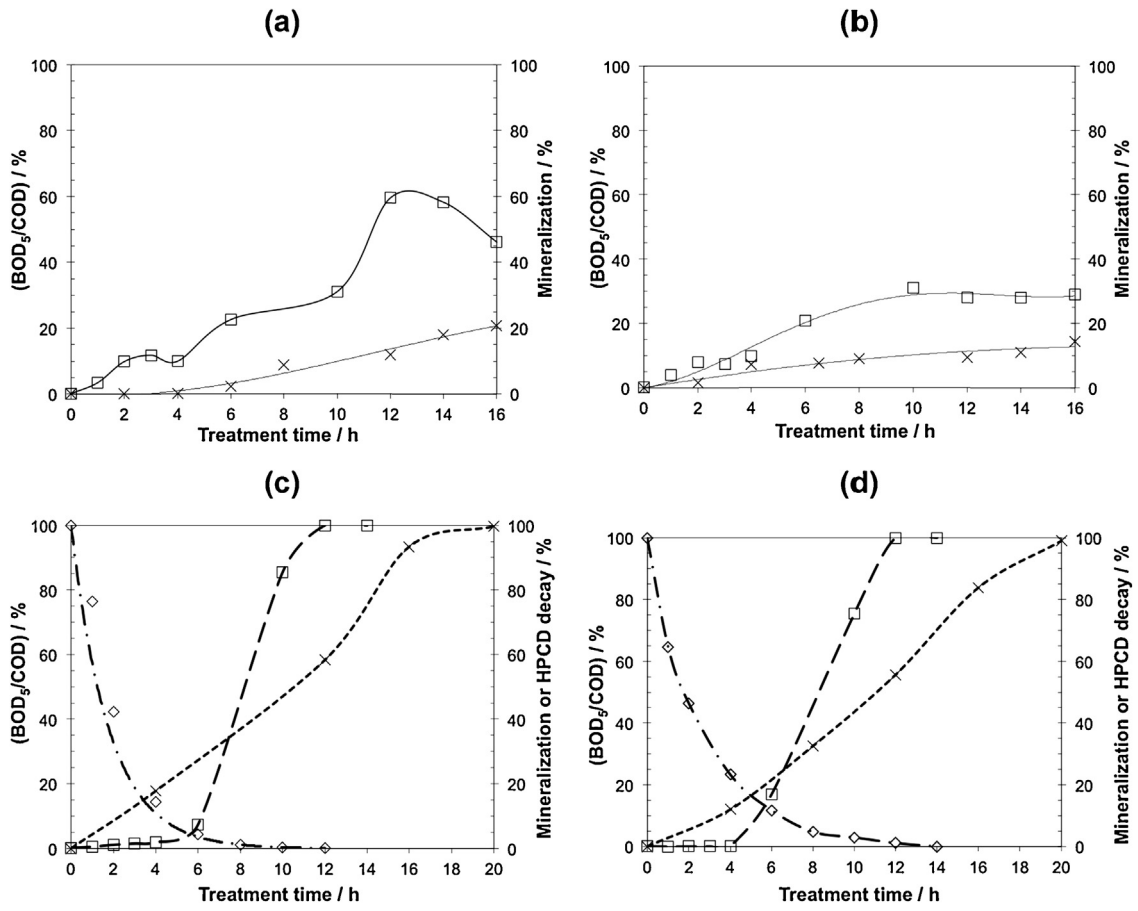

Fig. 4. Biodegradability assessment (BOD_5/COD ratio) (□), mineralization rate (×) and HPCD decay (◊) during EF or AO degradation of PHE (0.09 mM) in the presence of HPCD (9 g L^{-1}) with different kind of anode materials: EF-Pt (a), EF-DSA (b), EF-BDD (c), AO-BDD (d), at constant applied current intensity of 1000 mA.

behaviour during EF degradation of sulfamethazine solutions (Pharmaceutical).

3.4. Comparison of toxicity during PHE and HPCD oxidative treatments

Evolution of the acute toxicity of treated synthetic soil washing solution during EF and AO degradation of PHE in the presence of HPCD with Pt, DSA and BDD anodes was investigated and results are given in Fig. 5 in which the toxicity is expressed in inhibition percentage of luminescence of bacteria *Vibrio fischeri* measured by Microtox® method. This figure shows that the initial percentage of inhibition is around 45%, which is due to the presence of PHE since the initial percentage of inhibition with HPCD alone is close to 0% [55]. Moreover, the solution toxicity became about 40% higher than the initial toxicity value during 10 h treatment (between 85 and 99% of inhibition), whatever the anodes employed. This is probably due to the formation of highly toxic oxidation by-products during electrolysis that are often observed in other works [10,60,64]. This intermediates could be due to the presence of PAH, since a recent study denotes the fact that hydroxylated PAH and particularly hydroxylated PHE have reprotoxic effect on carps [65]. This high toxicity can be also due to the by-products formed through HPCD oxidation and mediated oxidation from electrolyte (persulfate and sulfate radicals) especially when BDD anode is employed [10,23]. The toxic oxidized compound formation can confirm the quick increase of toxicity at the beginning of the treatment. However, the toxicity during the first 4 h of treatment (time to degrade PHE) is higher (99%) with BDD than with DSA and Pt (85–90%) anodes. That means that different oxidation/mineralization kinetics were involved according to the anode used, and the quicker formation of toxic intermediates observed with BDD anode can be explained by the rapid formation of hydroxylated and/or quinone form derivatives involved with this anode (see Section 3.1.2). Toxicity obtained with EF-DSA treatment is constant and is still high even after 16 h treatment. During EF-Pt process, the toxicity starts to decrease after 10 h of treatment. However the mineralization yield is still low even after 16 h (20%) and the treatment is not accomplished yet at this time. In that way, it is possible that the toxicity restarts to increase after the 16 h of treatment. Regarding the treatments with BDD anode, after reaching 60% of mineralization (at 12 h), all the HPCD is degraded and the solution toxicity started to decrease until the complete mineralization (20 h) in both treatments. The quicker decrease with EF-BDD could be due to the paired electrocatalysis process (see Section 3.1.2).

By comparing with biodegradability data, the toxicity is higher and BOD_5 is lower with EF-BDD and AO-BDD processes, and the mineralization degree (inversely related to COD) is still too low, at the beginning of the treatment. After 6 h treatment, the biodegradability of synthetic soil washing solution increases very quickly when using BDD as anode. At this time the toxicity is still high and the BOD_5 is lower than with Pt and DSA, but the mineralization of organic compounds of synthetic soil solution increases very quickly in the meanwhile. The solutions treated with Pt anode are less toxic after 10 h treatment and its biodegradability increases quickly, even if the mineralization is low (around 10–15%). After 13 h, the mineralization yield is still low (15–20%) and the BOD_5 decreases slightly even if the toxicity decreases. Apparently, some less biodegradable or more toxic by-products are formed. Regarding DSA experiments, the mineralization rate increases slowly and the toxicity is still

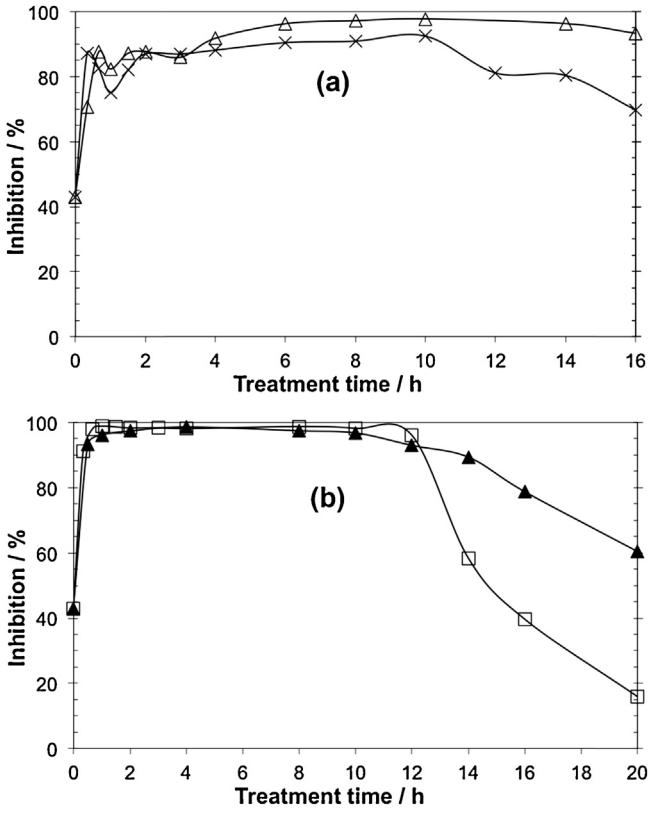

Fig. 5. Toxicity evolution after 15 min of exposure to *Vibrio fischeri* bacteria during EF or AO degradation of PHE (0.09 mM) in the presence of HPCD (9 g L^{-1}) with different kind of anode materials, at constant applied current intensity of 1000 mA: (a) EF-Pt (×), EF-DSA (△); (b) EF-BDD (□), AO-BDD (▲).

higher after 10 h of treatment. Thus, toxicity results are in agreement with those obtained in Section 3.1.

3.5. Comparison of the different treatments efficiency and their relative energy consumption

Since an effluent with a BOD_5/COD ratio higher than 33% is considered as biodegradable in industrial wastewater treatment [58], a biological post-treatment could be considered after reaching this threshold with EF process. Fig. 6 illustrates radar diagrams comparing different ways to combine EF with or without a biological post-treatment. The numerical values corresponding to Fig. 6 were given in Table 3.

The first option would be to do a biological treatment after reaching a maximal biodegradability ratio with EF treatment. The second one is to combine with a biological post-treatment after reaching the threshold value (33%). The last suggested solution would be to run EF treatment until the complete mineralization. The following parameters are taken into account: time of treatment, mineralization rate, biodegradability (%), toxicity (% of inhibition of luminescence), energy consumption per volume of solution treated (kWh m^{-3}) (Eq. (6)), and energy consumption per unit TOC mass removed (kWh (kg TOC)$^{-1}$) (Eq. (7)).

At maximal biodegradability ratio, the treatments with BDD anode have better efficiency compared to EF-Pt and EF-DSA in terms of mineralization, biodegradability and energy consumption per unit TOC mass. The energy consumption per volume with BDD anode is higher than with Pt and DSA anodes because of high O_2 overpotential the former anode, which increases E_{cell} value, a parameter of energy consumption in Eqs. (6) and (7).

Table 3
Comparison of EF (with Pt, DSA or BDD anodes) and AO-BDD processes. Six parameters are taken into account by considering three different ways of treatment.

	Time of treatment (h)				Mineralization yield (%)				Biodegradability (BOD_5/COD)(%)				Toxicity (Inhibition)(%)				Energy consumption per volume (kWh m^{-3})[a]				Energy consumption per TOC (kWh (kg TOC)$^{-1}$)[a]			
	EF-Pt	EF-DSA	EF-BDD	AO-BDD	EF-Pt	EF-DSA	EF-BDD	AO-BDD	EF-Pt	EF-DSA	EF-BDD	AO-BDD	EF-Pt	EF-DSA	EF-BDD	AO-BDD	EF-Pt	EF-DSA	EF-BDD	AO-BDD	EF-Pt	EF-DSA	EF-BDD	AO-BDD
Maximal biodegradability ratio	13	10	12	12	15	8	58	56	60	33	100	100	81	89	92	93	142	111	193	177	232	329	60	69
33% of biodegradability ratio	10	10	7	7	10	9	25	25	33	33	33	33	90	95	96	98	109	111	96	103	258	329	94	90
Complete mineralization	–	–	20	20	–	–	99.7	99.0	–	–	0	0	–	–	16	60	–	–	275	295	–	–	59	65

[a] Only electrical energy supplied for electrolysis is considered.

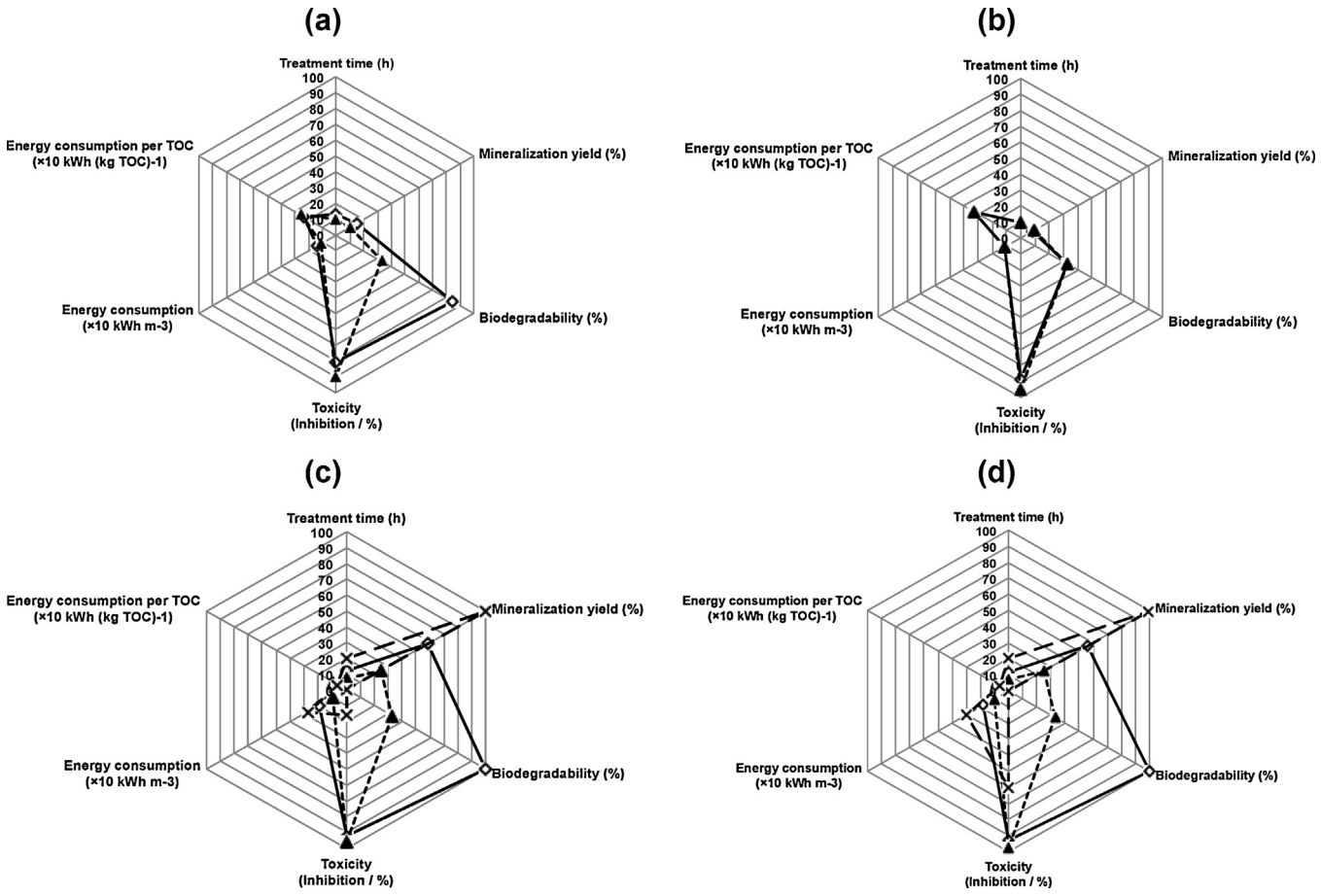

Fig. 6. Comparison of different treatments efficiency such as EF-Pt (a), EF-DSA (b), EF-BDD (c) and AO-BDD (d) by taking into account six parameters: time of treatment, mineralization yield, biodegradability (%), toxicity (% of inhibition), energy consumption per volume ($kWh\,m^{-3}$), energy consumption per unit TOC mass removed ($kWh\,(kg\,TOC)^{-1}$). Three treatments conditions are suggested: maximal biodegradability ratio (◊), 33% of biodegradability (▲) and complete mineralization (×).

At the threshold value that allows considering a biological post-treatment, EF-BDD and AO-BDD have shown better effectiveness by taking into account all the six parameters. Indeed, only 7 h (corresponding to 25% mineralization) of BDD treatments is required to reach 33% of biodegradability against 10 h (corresponding to around 10% mineralization) with Pt and DSA treatments. This leads to slightly better energy consumption per volume and largely better energy consumption per TOC. The toxicity is higher than 90% in all kinds of treatments. Even if EF-Pt gives similar values of energy consumption per volume as BDD treatments, the energy consumption per TOC and the mineralization remain still low.

Regarding the treatments until the complete mineralization, only processes with BDD are compared. EF-Pt and EF-DSA treatments demonstrated to have too slow mineralization rate to be run until the complete mineralization. EF-BDD and AO-BDD processes show similar efficiency with all the parameters, tough the toxicity is higher in the case of AO-BDD.

Treatments until complete mineralization are similar to treatments at maximal biodegradability ratio for EF-BDD and AO-BDD processes in terms of energy consumption per TOC. In both case, energy consumption is between 2 and 3 times higher than for BDD treatments until 33% of biodegradability. Thus, by comparing the three different ways suggested with BDD treatments, the treatment until 33% of biodegradability appears to be a good compromise between energy consumption per volume and energy consumption per TOC. Besides, EF-BDD and AO-BDD have similar behaviour in all cases. EF-Pt and EF-DSA processes have shown less conclusive results than treatments with BDD anode, whatever the way suggested.

Moreover, knowing that the cost of Pt material is much higher than BDD and DSA ones, it appears meaningful to consider BDD in a larger study scale as the best choice as anode of electrochemical advanced oxidation. Since iron is often present in soil, soil washing solution enhanced by an extracting agent like HPCD could have soluble iron. In that case, EF-BDD treatment would be suggested as the best option compared to EF-Pt and EF-DSA processes.

4. Conclusions

This study shows that anode materials play an important role in the treatment by EAOPs of synthetic soil washing solutions containing PHE and HPCD in terms of concentration decay kinetics, mineralization, biodegradability, toxicity and energy consumption. The oxidizing agent •OH can be generated in the in the bulk solution (from Fenton's reaction) and/or at the surface of a high-O_2 overvoltage electrode like BDD. Thus, Pt and DSA electrodes favour the oxidative degradation mechanism (generation of •OH in the bulk solution) through EF process while AO-BDD promotes mineralization, and EF-BDD supports both ways. These results are confirmed by the time-course of PHE and HPCD decay as well as the biodegradability and toxicity assays. Competitive decay between PHE and HPCD are observed. EF-BDD and AO-BDD give largely better TOC decay than EF-Pt and EF-DSA. During BDD treatments, the mineralization increases linearly when the applied current increases from 0 to 2000 mA. It permits to note that EF-BDD is 1.35 times better than

AO-BDD to mineralize synthetic soil washing solutions. At 1000 mA, the complete mineralization is achieved after 20 h of EF-BDD and AO-BDD treatments. In AO-BDD, the toxicity starts to decrease and the biodegradability reaches a maximum value (100%) when the degradation of initial compounds (PHE and HPCD) is achieved (at about 60% of mineralization). Due to this fact the best condition to increase the biodegradability of the sample will be high removal rate of HPCD from solution.

A minimum biodegradability ratio of 33% is taken into account to consider a biological post-treatment. Six parameters (the time of treatment, the mineralization yield, the biodegradability, the toxicity, the energy consumption per volume and the energy consumption per TOC) are taken into account to compare the electrochemical treatment until 33% of biodegradability, until maximal biodegradability ratio and until the complete mineralization. Considering a pre-treatment with EF-BDD or AO-BDD until reaching a biodegradability of 33% seems to be a good compromise. As the Pt electrode is more expensive than DSA and BDD ones the use of this anode at industrial scale is ruled out. These results give a promising methodology to perform further experiments with soil washing solution from a historically PAHs-contaminated soil.

Acknowledgements

The authors would like to thank the organizations that provided financial support: (i) The University of Paris-Est and (ii) the European Commission through the Erasmus Mundus Joint Doctorate Programme ETeCoS^3 (Environmental Technologies for Contaminated Solids, Soils and Sediments) under the grant agreement FPA n° 2010-0009.

References

[1] X.-T. Wang, Y. Miao, Y. Zhang, Y.-C. Li, M.-H. Wu, G. Yu, Sci. Total Environ. 447 (2013) 80–89.
[2] T.B. Boving, X. Wang, M.L. Brusseau, Environ. Sci. Technol. 33 (1999) 764–770.
[3] D. Landy, I. Mallard, A. Ponchel, E. Monflier, S. Fourmentin, Environ. Chem. Lett. 10 (2012) 225–237.
[4] E. Mousset, M.A. Oturan, E.D. van Hullebusch, G. Guibaud, G. Esposito, Crit. Rev. Environ. Sci. Technol. 44 (2014) 705–795.
[5] J. Gómez, M.T. Alcántara, M. Pazos, M.Á. Sanromán, Chem. Eng. J. 159 (2010) 53–57.
[6] W.H. Glaze, J.W. Kang, D.H. Chapin, Ozone Sci. Eng. 9 (1987) 335–352.
[7] W.M. Latimer, Soil Sci. 74 (1952) 333.
[8] M.A. Oturan, J.-J. Aaron, Crit. Rev. Environ. Sci. Technol. (2014), 140225124605005.
[9] M. Stylidi, D. Kondarides, X. Verykios, Appl. Catal. B: Environ. 40 (2003) 271–286.
[10] E. Brillas, I. Sirès, M.A. Oturan, Chem. Rev. 109 (2009) 6570–6631.
[11] M.A. Oturan, J. Appl. Electrochem. 30 (2000) 475–482.
[12] I. Sirés, E. Brillas, Environ. Int. 40 (2012) 212–229.
[13] M.A. Rodrigo, N. Oturan, M.A. Oturan, Chem. Rev. (2014) (in press).
[14] P. Cañizares, R. Paz, C. Sáez, M.A. Rodrigo, J. Environ. Manage. 90 (2009) 410–420.
[15] M. Zhou, Q. Yu, L. Lei, G. Barton, Sep. Purif. Technol. 57 (2007) 380–387.
[16] H. Zhang, D. Zhang, J. Zhou, J. Hazard. Mater. 135 (2006) 106–111.
[17] M. Zhou, Q. Tan, Q. Wang, Y. Jiao, N. Oturan, M.A. Oturan, J. Hazard. Mater. 215–216 (2012) 287–293.
[18] I. Sires, J. Garrido, R. Rodriguez, E. Brillas, N. Oturan, M.A. Oturan, Appl. Catal. B: Environ. 72 (2007) 382–394.
[19] N. Oturan, M. Zhou, M.A. Oturan, J. Phys. Chem. A 114 (2010) 10605–10611.
[20] P.V. Nidheesh, R. Gandhimathi, Desalination 299 (2012) 1–15.
[21] C.A. Martínez-Huitle, E. Brillas, Appl. Catal. B: Environ. 87 (2009) 105–145.
[22] E. Mousset, D. Huguenot, E.D. van Hullebusch, N. Oturan, G. Guibaud, G. Esposito, et al., Proceeding 12th AquaConSoil 2013 Int. Conf. Barcelona, Barcelona (Spain), 2013.
[23] M. Panizza, G. Cerisola, Chem. Rev. 109 (2009) 6541–6569.
[24] N. Oturan, E. Brillas, M.A. Oturan, Environ. Chem. Lett. 10 (2012) 165–170.
[25] S. Randazzo, O. Scialdone, E. Brillas, I. Sirés, J. Hazard. Mater. 192 (2011) 1555–1564.
[26] E. Brillas, C.A. Martinez-Huitle, Synthetic Diamond Films: Preparation, Electrochemistry Characterization and Applications, Wiley, New Jersey, 2011.
[27] M.A. Rodrigo, P.A. Michaud, I. Duo, M. Panizza, G. Cerisola, C. Comninellis, J. Electrochem. Soc. 148 (2001) D60–D64.
[28] J.A. Sánchez Pérez, I.M. Román Sánchez, I. Carra, A. Cabrera Reina, J.L. Casas López, S. Malato, J. Hazard. Mater. 244–245 (2013) 195–203.
[29] P. Cañizares, A. Beteta, C. Sáez, L. Rodríguez, M.a. Rodrigo, Chemosphere 72 (2008) 1080–1085.
[30] I. Oller, S. Malato, J.A. Sánchez-Pérez, Sci. Total Environ. 409 (2011) 4141–4166.
[31] S.H. Lin, C.D. Jiang, Desalination 154 (2003) 107–116.
[32] C.S.D. Rodrigues, L.M. Madeira, R.A.R. Boaventura, J. Hazard. Mater. 172 (2009) 1551–1559.
[33] R.C. Martins, A.F. Rossi, R.M. Quinta-Ferreira, J. Hazard. Mater. 180 (2010) 716–721.
[34] J.A. Zimbron, K.F. Reardon, Water Res. 45 (2011) 5705–5714.
[35] X.-J. Wang, Y. Song, J.-S. Mai, J. Hazard. Mater. 160 (2008) 344–348.
[36] M. Lapertot, C. Pulgarín, P. Fernández-Ibáñez, M.I. Maldonado, L. Pérez-Estrada, I. Oller, et al., Water Res. 40 (2006) 1086–1094.
[37] V.J.P. Vilar, E.M.R. Rocha, F.S. Mota, A. Fonseca, I. Saraiva, R.A.R. Boaventura, Water Res. 45 (2011) 2647–2658.
[38] E.S. Elmolla, M. Chaudhuri, J. Hazard. Mater. 192 (2011) 1418–1426.
[39] S. Malato, J. Blanco, M.I. Maldonado, I. Oller, W. Gernjak, L. Pérez-Estrada, J. Hazard. Mater. 146 (2007) 440–446.
[40] A. Serra, E. Brillas, X. Domènech, J. Peral, Chem. Eng. J. 172 (2011) 654–664.
[41] M.J. Farré, X. Doménech, J. Peral, J. Hazard. Mater. 147 (2007) 167–174.
[42] D. Mansour, F. Fourcade, N. Bellakhal, M. Dachraoui, D. Hauchard, A. Amrane, Water Air Soil Pollut. 223 (2012) 2023–2034.
[43] A.L. Estrada, Y.-Y. Li, A. Wang, J. Hazard. Mater. 227–228 (2012) 41–48.
[44] D. Mansour, F. Fourcade, S. Huguet, I. Soutrel, N. Bellakhal, M. Dachraoui, et al., Int. Biodeterior. Biodegrad. 88 (2014) 29–36.
[45] F. Ferrag-Siagh, F. Fourcade, I. Soutrel, H. Aït-Amar, H. Djelal, A. Amrane, J. Chem. Technol. Biotechnol. 88 (2013) 1380–1386.
[46] B. Balci, N. Oturan, R. Cherrier, M.A. Oturan, Water Res. 43 (2009) 1924–1934.
[47] A. Fernandes, P. Spranger, A.D. Fonseca, M.J. Pacheco, L. Ciríaco, A. Lopes, Appl. Catal. B: Environ. 144 (2014) 514–520.
[48] Y. Chu, D. Zhang, L. Liu, Y. Qian, L. Li, J. Hazard. Mater. 252–253 (2013) 306–312.
[49] I. Yahiaoui, F. Aissani-Benissad, F. Fourcade, A. Amrane, Chem. Eng. J. 221 (2013) 418–425.
[50] V.M. Daskalaki, H. Marakas, D. Mantzavinos, A. Katsaounis, P. Gikas, Water Sci. Technol. 68 (2013) 2344–2350.
[51] J.-M. Fontmorin, F. Fourcade, F. Geneste, D. Floner, S. Huguet, A. Amrane, Biochem. Eng. J. 70 (2013) 17–22.
[52] Y. Chen, L. Hong, W. Han, L. Wang, X. Sun, J. Li, Chem. Eng. J. 168 (2011) 1256–1262.
[53] Y.-Y. Chu, W.-J. Wang, M. Wang, J. Hazard. Mater. 180 (2010) 247–252.
[54] N. Oturan, J. Wu, H. Zhang, V.K. Sharma, M.A. Oturan, Appl. Catal. B: Environ. 140–141 (2013) 92–97.
[55] E. Mousset, N. Oturan, E.D. van Hullebusch, G. Guibaud, G. Esposito, M.A. Oturan, Water Res. 48 (2014) 306–316.
[56] P. Reuschenbach, U. Pagga, U. Strotmann, Water Res. 37 (2003) 1571–1582.
[57] M.M. Ballesteros Martín, J.L. Casas López, I. Oller, S. Malato, J.A. Sánchez Pérez, Ecotoxicol. Environ. Saf. 73 (2010) 1189–1195.
[58] J. Rodier, B. Legube, N. Merlet, Analyse de l'eau (Water Analysis), ninth, Dunod, Paris, 2009 (in French).
[59] M.M. Ballesteros Martín, J.A. Sánchez Pérez, F.G. Acién Fernández, J.L. Casas López, A.M. García-Ripoll, A. Arques, et al., Chemosphere 70 (2008) 1476–1483.
[60] A. Dirany, S. Efremova Aaron, N. Oturan, I. Sirés, M.A. Oturan, J. Aaron, Anal. Bioanal. Chem. 400 (2011) 353–360.
[61] K. Hanna, S. Chiron, M.A. Oturan, Water Res. 39 (2005) 2763–2773.
[62] X. Wang, M.L. Brusseau, Environ. Sci. Technol. 27 (1993) 2821–2825.
[63] K. Cruz-González, O. Torres-Lopez, A.M. García-León, E. Brillas, A. Hernández-Ramírez, J.M. Peralta-Hernández, Desalination 286 (2012) 63–68.
[64] A. Dirany, I. Sirés, N. Oturan, A. Ozcan, M.A. Oturan, Environ. Sci. Technol. 46 (2012) 4074–4082.
[65] D. Fernandes, C. Porte, Sci. Total Environ. 447 (2013) 152–159.